Colloid & Polymer Science Colloid Polym Sci 272:554–561 (1994)

Lyotropic effect in surface charge, electrokinetics, and coagulation of a rutile dispersion

N. Kallay, M. Čolić[1]), D.W. Fuerstenau[1]), H.M. Jang[1]), and E. Matijević[2])

Laboratory of Physical Chemistry, Faculty of Science, University of Zagreb, Zagreb, Croatia
[1]) Department of Materials Science and Mineral Engineering, University of California, Berkeley, California, USA
[2]) Center for Advanced Materials Processing, Clarkson University, Potsdam, New York, USA

Abstract: Potentiometric, electrokinetic, and coagulation experiments with a rutile dispersion in the pH region above the point of zero charge exhibit an "inverse" lyotropic sequence for counterions: $Li^+ > K^+ > Cs^+$. The potentiometric and electrokinetic data were interpreted by a surface complexation model assuming the Stern–Gouy–Chapman structure of the interfacial layer, which yielded the values of inner layer capacitances, C, and the intrinsic equilibrium constants, K^0_{ass}, characterizing the specificity of each counterion. These parameters were used to explain the order of lyotropic sequences in the adsorption, coagulation, and electrokinetic phenomena.

Key words: Coagulation – electrokinetics – interfacial layer – lyotropic effect – rutile

Introduction

The lyotropic effect [1–3], which can be observed in the adsorption of ions, electrokinetic, coagulation, adhesion phenomena, etc., indicates a significant role of ionic interactions in the inner part of the electrical interfacial layer, where amphoteric surface equilibria and counterion association with surface charged groups can take place. In most cases ions of larger crystallographic radii show greater tendency towards surface binding (adsorption); thus, they reduce more efficiently the electrokinetic potential and exhibit lower critical coagulation concentrations (ccc).

The simple explanation of the "regular" lyotropic sequence is based on the hydration: ions of smaller crystallographic radii bind water molecules more strongly and, being effectively larger, they cannot approach the surface charged groups as closely as smaller species, resulting in a weaker electrostatic attraction. In treating the association of two ions of opposite charge one should take into account the (center-to-center) distance of closest approach, which is not a simple sum of their radii [4–7]. The superimposed electrical fields may influence the structure of the surrounding water and, consequently, the distance of the closest approach, which may explain inverse lyotropic sequences. For example, Mg^{2+}, which has a smaller crystallographic radius than Ba^{2+} but is larger in the "effective size" when hydrated, showed higher adsorption affinity for Al_2O_3 [8]. For AgI, As_2S_3, MnO_2, SiO_2, etc., dispersions the lyotropic order was found to be "regular" [1]. Dumont, Warlus, and Watillon [2] suggested that the "inverse" sequence applied to surfaces of high heat of immersion, that is, to surfaces which chemisorb water. The order may depend on the preparation and the treatment of the sample, as has been demonstrated with TiO_2 [2]. A possible electroviscous effect, considered by Warszyński and van de Ven [9], would only lead to a more or less pronounced "regular" sequence, but could not explain the "inverse" order.

The surface complexation model [10–15] accounts for the counterion specificity through two parameters:

i) The first parameter is the capacitance of the inner layer capacitor (C), consisting of the 0-plane in which the surface charged groups are located, and the d-plane in which counterion association takes place. Since the distance between these two planes and the structure of water in this region (actual permittivity) depend on the nature of the counterions, one would expect a characteristic C value for each case. Normally, the effectively smaller counterions should produce a higher C value.

ii) The second parameter is the intrinsic equilibrium constant for counterion association (K^0_{ass}). For indifferent electrolytes, the latter is mainly determined by the electrostatic interaction between a surface charged group and the counterion. In this case the charge of the counterion dominates, while its size is of lesser significance. Still, the smaller the counterion, the closer it will approach the surface charged group, resulting in a stronger coulombic attraction and a larger value of K^0_{ass}.

The process of binding the counterions to the surface charge groups (MOH_2^+ and MO^-) is characterized by three contributions: i) the electrostatic attraction between the surface charge groups and counterions (coulombic attraction), ii) electrostatic attraction of counterions by all other statistically distributed ions at or near the surface, and iii) chemical bonds formations.

The contribution ii) does not apply at the zero point of charge (zpc), and the binding of ions of an indifferent electrolyte is rather weak, eliminating case iii). Thus, the total equilibrium constant is essentially determined by interactions i).

The aim of this work is to examine the lyotropic sequence of alkali cations for rutile through potentiometric (adsorption), electrokinetic, and coagulation measurements and to interpret the results on the basis of the above-mentioned parameters (C, K^0_{ass}). The significance of this approach is in the use of three different techniques in order to gain the necessary information for the interpretation of data.

Experimental

Materials

The sample of rutile (TiO_2) (Tioxide International Ltd., Cleveland, England, Code Number CLDD 1597) was prepared by the hydrolysis of redistilled titanium chloride, followed by heating in air at 450 °C for 2 h. Since the pH of the aqueous suspension, as received, was 4 and a considerable amount of chloride ions was retained on the surface, the sample was carefully purified. The excess of the acid was neutralized with sodium hydroxide and the supernatant solution was replaced after 24 h. This washing procedure was repeated 10 times, and then the sample was dialyzed for 2 months until no sodium or chloride ions could be detected by atomic absorption and by the silver nitrate test, respectively. Electron micrographs showed particles to be rod-like with the length ranging from 0.1 to 0.24 μm and the width of 0.045 ± 0.010 μm. The BET specific surface area was 21 $m^2 g^{-1}$. All chemicals used in this work were of analytical grade and the solutions were kept under argon.

Potentiometric titration

Potentiometric titrations of suspensions, containing 1 g of solid per 100 cm^3 of solution, were carried out under argon atmosphere at 25.0 °C using a Fischer glass electrode with a negligible sodium error (pH range 0–14). The reference calomel electrode was connected by a salt bridge of the same electrolyte composition as the titrated system. The electrodes were calibrated by a blank titration, in the absence of suspended solids, as described elsewhere [16, 17]. The surface charge densities at the 0-plane (σ_0) were calculated from titration curves by the usual procedure [18]. The point of zero charge (pzc) was obtained from the common intersection point of the σ_0(pH) functions at different ionic strengths and was always located at pH = 6.0.

Electrokinetics

The electrophoretic mobilities of suspended particles were determined with the PenKem 501 Zetameter with samples equilibrated for 30 min before measurements. The isoelectric point (iep) was found at pH = 6.0, which agreed with the pzc value, indicating the absence of any specific adsorption.

Coagulation

Critical coagulation concentrations (ccc) of several electrolytes were determined by the common light scattering method as described earlier [3].

Results

The results of the potentiometric titrations are presented in Figs. 1 and 2, where the surface charge density at 0-plane (σ_0), as calculated from the adsorption density of hydrogen/hydroxyl ions, is plotted as a function of the pH. As expected, the values of σ_0 are always greater at higher electrolyte concentrations. The specific influence of different anions is seen only below the pzc, because the surface bears positively charged groups which associate with Cl^-, NO_3^-, or ClO_4^- (Fig. 1), while the effect is negligible at pzc. An analogous finding was observed with cations (Fig. 2) above the pzc. The affinity towards association (higher affinity → higher σ_0) follows the sequence:

$$Li^+ > K^+ > Cs^+ \quad \text{and}$$

$$Cl^- > NO_3^- > ClO_4^-$$

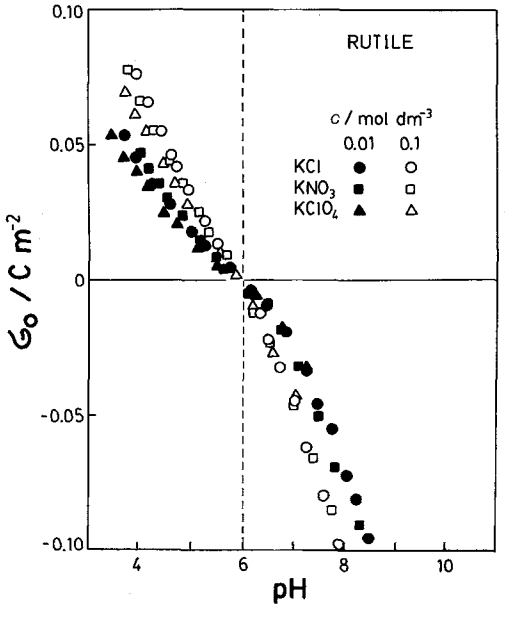

Fig. 1. The surface charge density (σ_0) of an aqueous rutile dispersion as a function of the pH at 25 °C in the presence of KCl (●, ○), KNO_3 (■, □), and $KClO_4$ (▲, △). The full and open symbols correspond to the ionic strength of $I = 0.01$ and 0.1 mol dm^{-3}, respectively

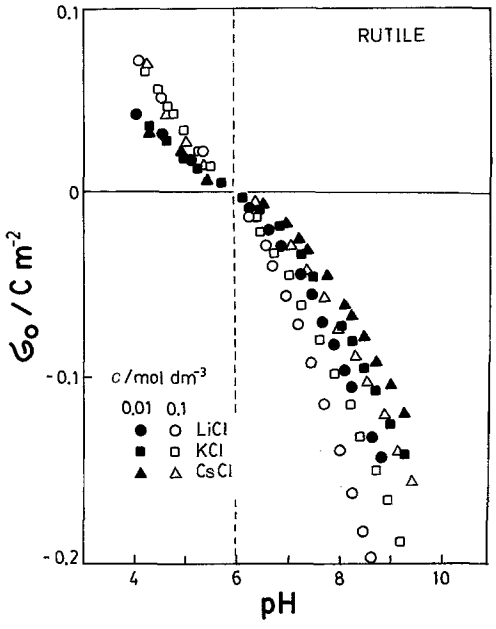

Fig. 2. The same plot as Fig. 1 for LiCl (●, ○), KCl (■, □), and CsCl (▲, △).

Figure 3 shows that the electrokinetic ζ-potentials as a function of the pH for different alkaline chlorides exhibit the lyotropic effect above the pzc. The higher affinity towards association results in lower ζ-potentials and the obtained order agrees with the adsorption data (Fig. 2).

Coagulation experiments yielded the same trend; the critical coagulation concentrations at pH = 10 for LiCl, KCl, and CsCl were found to be 0.039, 0.060, and 0.136 mol dm^{-3}, respectively.

Interpretation

The "simultaneous" interpretation of potentiometric and electrokinetic data, based on the surface complexation–Stern–Gouy–Chapman model (scSGC), was carried out as described earlier [3]. The treatment assumes positive (MOH_2^+) and negative (MO^-) surface charged groups to be located at the 0-plane and the associated counterions at the *d*-plane, which is taken to be the onset (inner boundary) of the diffuse layer described by the Gouy–Chapman theory. The total surface concentration of active amphoteric surface sites (Γ_{tot}) was chosen to be 10^{-5} mol m^{-2} (see refs. [19, 20]), while other

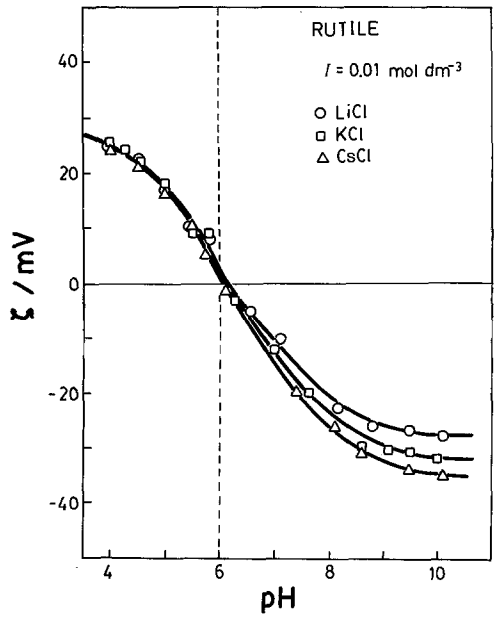

Fig. 3. The electrokinetic potential of rutile particles as a function of the pH at 25 °C in the presence of 0.01 mol dm^{-3} of LiCl (○), KCl (□), and CsCl (△)

parameters were $T = 298$ K, $\varepsilon_r = 78.5$, and $pH_{pzc} = 6$. The electrokinetic slipping plane was assumed to be separated by 12 Å from the *d*-plane [17], the value of which influences some constants but does not affect the general conclusions of this work.

The applied method makes it possible to calculate the parameters of surface equilibria. The electrokinetic mobilities yield the ψ_d potentials at the onset of the diffuse double layer, as well as the charge density of the latter. These data combined with the results of the potentiometric titrations are used to evaluate other quantities related to equilibria.

The interpretation of data for rutile in the presence of KCl gave the most consistent intrinsic equilibrium constant for the formation of positive surface sites:

$$MOH + H^+ \rightleftarrows MOH_2^+; \quad K_a^0 = 6 \cdot 10^7 , \quad (1)$$

where

$$K_a^0 \exp(-e\psi_0/kT) = \{MOH_2^+\}/\{MOH\}a_{H^+} \quad (2)$$

ψ_0 being the potential at the 0-plane and { } designate surface concentrations.

Since pH_{pzc} was found to be 6.0,

$$MOH \rightleftarrows MO^- + H^+; K_b^0 = 6 \cdot 10^{-5} , \quad (3)$$

with

$$K_b^0 \exp(e\psi_0/kT) = \{MO^-\}a_{H^+}/\{MOH\} . \quad (4)$$

The intrinsic equilibrium constant for the association of potassium ions with negatively charged surface groups was calculated as

$$MO^- + K^+ \rightleftarrows MOK; K_{ass}^0(K^+) = 125 , \quad (5)$$

with

$$K_{ass}^0(K^+) \exp(-e\psi_\beta/kT) = \{MOK)/\{MO^-\}a_{K^+} , \quad (6)$$

where ψ_β is the electrokinetic potential at the β-plane in which are located associated counterions. For other two cations: $K_{ass}^0(Li^+) = 380$ and $K_{ass}^0(Cs^+) = 51$.

The inner layer capacitance (per unit surface area) defined as

$$C = \sigma_0/(\psi_0 - \psi_d) \quad (7)$$

was found to be

$$C(K^+) = 1.15 \text{ F m}^{-2}, \; C(Li^+) = 1.58 \text{ F m}^{-2},$$

and $C(Cs^+) = 1.08$ F m^{-2} .

Discussion

The rutile sample used in this study showed the "inverse" lyotropic series in the surface charge, electrokinetic, and coagulation phenomena. The same sequence for TiO_2 was found by Bérubé and de Bruyn [21] and Sprycha [22], while Dumont, Warlus, and Watillon [2] obtained both "regular" and "inverse" orders, depending on the preparation and the treatment of the rutile sample. The latter authors explained the observed effects on the basis of the "structure-making" behavior, which is characteristic of surfaces with high heats of immersion.

The two critical parameters (C and K_{ass}^0), characterizing the counterion/surface site interactions are interrelated, and should follow the same lyotropic sequence. For "effectively smaller" ions, the distance between the 0- and *d*-planes (d) is shorter and, therefore, the C values must be higher.

$$C = \varepsilon_0 \varepsilon_r / d . \quad (8)$$

The K^0_{ass} value should also be larger for "smaller" ions, which can approach the center of a surface charged group more closely, due to the stronger electrostatic attraction. Since the overall electrostatic potential does not contribute to the value of K^0_{ass}, the lyotropic effect may be analyzed in terms of two contributions to the standard Gibbs energy change of association (ΔG^0_{ass}):

i) The coulombic part, ΔG^0_C, due to electrostatic forces between interacting ions at distance d. For a pair of ions of charge numbers $+1$ and -1

$$\Delta G^0_C = -\frac{N_A e^2}{4\pi\varepsilon_0\varepsilon_r d} \qquad (9)$$

(N_A is the Avogadro constant and e is the proton charge), and

ii) The "chemical" part, ΔG^0_{ch}, representing contributions other than the coulombic. (For indifferent electrolytes, ΔG^0_{ch} is expected to be zero.) Thus,

$$-RT\ln K^0_{ass} = \Delta G^0_{ass} = \Delta G^0_{ch} + \Delta G^0_C$$

$$= \Delta G^0_{ch} - \frac{N_A e^2}{4\pi\varepsilon_0\varepsilon_r d}. \qquad (10)$$

The expression (9) is approximate. Alternately, it is possible to calculate the statistical distribution of counterions surrounding surface charge groups in accordance with the Bjerrum concept as shown in refs. [6, 7].

Note that the electrostatic contribution due to the electrical double layer does not affect the intrinsic equilibrium constant. Equation (8) and (10) yield

$$\ln K^0_{ass} = -\frac{\Delta G^0_{ch}}{RT} + \frac{N_A e^2}{RT4\pi\varepsilon_0^2\varepsilon_r^2}\cdot C\,. \qquad (11)$$

Figure 4 is plot of log K^0_{ass} as a function of C for various investigated cations on rutile. For comparison, the results for anions interacting with hematite surface [3] are also included. It is clear that Li^+, showing the strongest lyotropic effect, is characterized by the highest K^0_{ass} and C values. A value of $\varepsilon_r = 78$ (dashed line) does not yield the experimental slope; instead, the reduced permittivity of the inner double layer region (between the 0- and d-planes) of $\varepsilon_r \approx 40$ fits the data. However, for the diffuse part of the interfacial layer $\varepsilon_r = 78.5$ still applies. The plot with $\varepsilon_r \approx 40$ also gives the

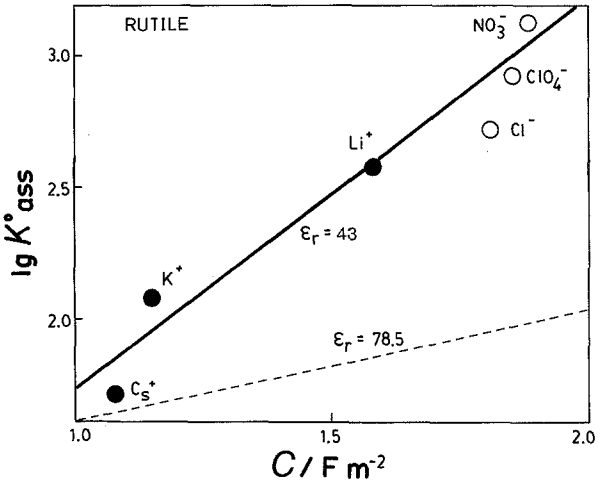

Fig. 4. The relationship between the intrinsic association constant (K^0_{ass}) and the inner layer capacitance (C) for rutile water interface at 25 °C as obtained with Cs^+, K^+, and Li^+ (filled symbols). Open symbols represent the same relationship for Cl^-, ClO_4^-, and NO_3^- at hematite interface (ref. [3]). The lines were calculated using Eq. (11) for $\varepsilon_r = 43$ (solid line) and $\varepsilon_r = 78.54$ (dashed line)

intercept $\Delta G^0_{ch} \approx 0$, which is consistent with the assumption that alkaline chlorides act as "indifferent electrolytes", i.e., no chemical bonding takes place. The data for anions on the hematite surface [3] fall on the same line, which may be just a coincidence.

Accepting the value of $\varepsilon_r = 43$, the distances of the closest approach, calculated using Eq. (8), and $d(Li^+) = 2.4$ Å, $d(K^+) = 3.3$ Å, and $d(Cs^+) = 3.5$ Å, in line with the Bjerrum theory of ion pairing [5–7]. These values of d are smaller than the Bjerrum critical distance for ion pairs in bulk solution, indicating that the association at the solid/liquid interface also takes place at the pzc in the absence of a superimposed electrical field of the "double layer", as is inherent in the definition of K^0_{ass} [Eq. (5)].

The parameters characterizing the equilibria in the electrical interfacial layer (Γ_{tot}, K^0_a, K^0_b, K^0_{ass}, and C) make it possible to estimate the critical coagulation concentration (ccc), by assuming a value of the Hamaker constant A. The van der Waals dispersion interaction energy was calculated by neglecting retardation effects [23], while the electrostatic contribution was evaluated using the Hogg, Healy, and Fuerstenau equation [24] for the constant potential. The latter was

found to better represent interactions in the liquid media than the assumption of constant charge [25]. The particles were considered as spheres of equivalent radius $r = 0.04\ \mu m$, which did not influence the calculated ccc values, but it affected the slope of the log stability factor, lg W, versus the log electrolyte concentration, lg C, plot. First, the potential at the inner boundary of the diffuse layer (Stern potential, ψ_d) was calculated for pH = 10 as a function of LiCl, KCl, and CsCl concentrations using the equilibrium parameters as obtained in this work. With these ψ_d values the heights of the maxima of the total interaction energy as a function of distance, E_{max}, were obtained, which were then used to generate the stability factor, W, since

$$W \approx \exp(E_{max}/kT)\,. \tag{12}$$

This expression is a good approximation for the evaluation of the ccc, because for rapid coagulation $E_{max} \to 0$ and $W \to 1$, but it is approximate for $W > 1$. The Hamaker constant $A = 6.2 \cdot 10^{-20}$ J, that fits the ccc of KCl, is in agreement with other published data [23]. With this value of A, the stability factor for rutile was obtained as a function of the concentration of LiCl, KCl, and CsCl (Fig. 5). The experimental ccc are denoted by arrows, except for Cs^+, the value of which is off scale. The calculated W functions follow the lyotropic order; the discrepancy in the ccc for Cs^+ is due to the high electrolyte concentration, because the deviations from the model are more pronounced.

The surface complexation approach, together with the Stern–Gouy–Chapman description of the structure of the interface, offer an additional explanation for different orders in the lyotropic series. Effectively smaller ions are characterized by higher C and K^0_{ass} values. While larger K^0_{ass} is directly connected with a higher counterion association affinity (consequently higher σ_0 and lower ζ and ccc values), the larger C may act in the opposite direction, since it represents a steeper potential drop between the 0- and d-planes [Eq. (7)]. The total surface association equilibrium constant (K_{ass}) and, consequently, the surface concentration of associated counterions (Γ_{MOK}) decreases, as is apparent from the expression

$$K_{ass}(K^+) = K^0_{ass}(K^+)\exp(-e\psi_d/kT) = \Gamma_{MOK}/\Gamma_{MO^-}a_{K^+}, \tag{13}$$

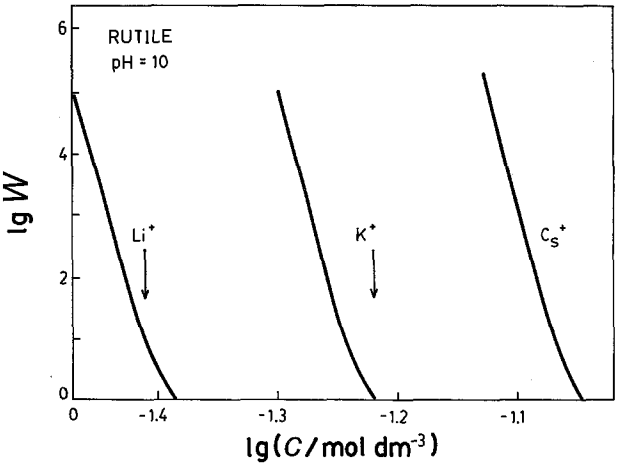

Fig. 5. The theoretical stability factor for a rutile dispersion as a function of LiCl, KCl, and CsCl concentrations. The parameters used in calculations are: 25 °C; pH = 10, $pH_{pzc} = 6$; $K^0_a = 6 \cdot 10^7$; $r = 0.04\ \mu m$; $A = 6.2 \cdot 10^{-20}$ J; $\Gamma_{tot} = 10^{-5}$ mol m^{-2}; $K^0_{ass} = 380\ (Li^+)$, 125 (K^+), 51 (Cs^+); C/F m^{-2} = 1.58 (Li^+), 1.15 (K^+), 1.08 (Cs^+). The arrows denote experimental ccc values, except for Cs^+ which is off scale

which was written for K^+ as the counterion. The dependence of the ccc on K^0_{ass} and C is illustrated in Fig. 6. In the upper part of this figure, the capacitance $C = 1.15$ F m^{-2} (as determined for K^+) was kept constant, while K^0_{ass} was varied to cover the range from 51 (for Cs^+) to 380 (for Li^+). As expected, the ccc decreases significantly as K^0_{ass} increases, pointing to the role of counterion association in colloid stability phenomena. The lower part of Fig. 6 demonstrates the effect of the variation of C (from 1.0 to 1.6 F m^{-2}) on the ccc using a constant $K^0_{ass}(K^+) = 115$. This range of C covers the values for Cs^+ (1.08 F m^{-2}) and Li^+ (1.58 F m^{-2}). It is clear that the ccc increases (i.e., coagulation ability decreases) as C becomes larger.

The above findings lead to the conclusion that the decrease in the effective counterion size, which is accompanied by an increase in both C and K^0_{ass}, has a two-fold effect on their coagulation ability. With larger K^0_{ass} the coagulation efficiency is enhanced, while a simultaneous increase in C reduces the ability of the counterions to compensate the charge effects and destabilize the system. For the rutile dispersion studied in this work, the influence of the counterion size on K^0_{ass} prevailed, although the opposite should be possible in some other case.

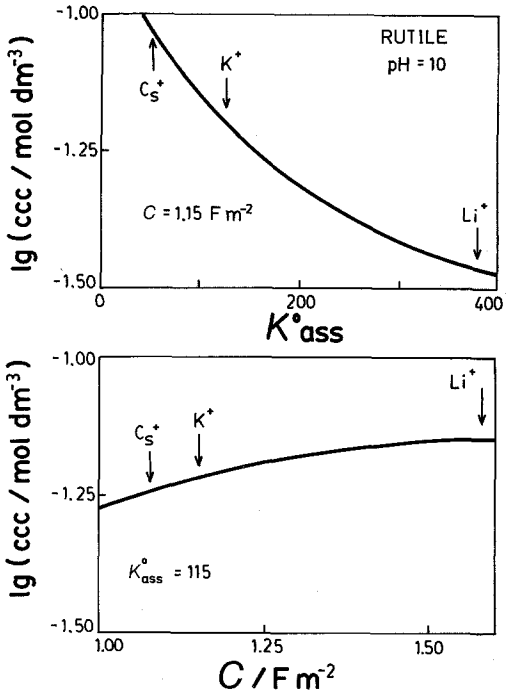

Fig. 6. Upper: The effect of intrinsic counterion association equilibrium constant, K^0_{ass}, on the critical coagulation concentration, ccc, for a rutile dispersion at constant inner layer capacitance $C = 1.15\,F\,m^{-2}$. Lower: The effect of the capacitance C on the ccc for the same system at constant K^0_{ass}. The arrows indicate K^0_{ass} (upper) and C (lower) values of Li^+, K^+, and Cs^+. In both plots all other parameters are the same as for Fig. 5

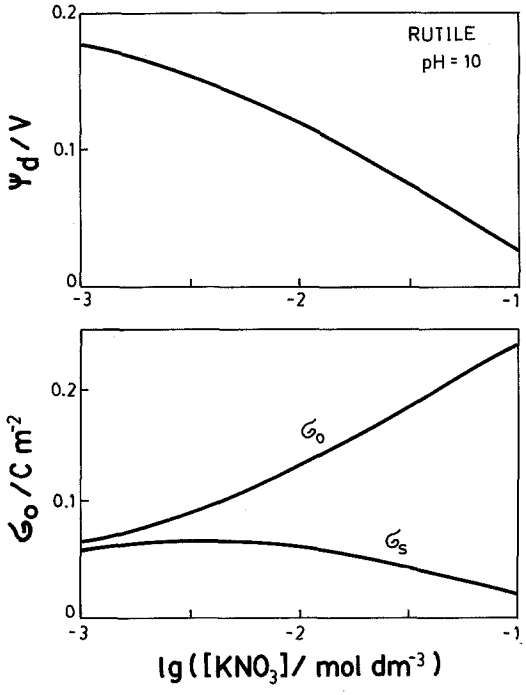

Fig. 7. The effect of KNO_3 concentration on the potential of the inner boundary of the diffuse layer, ψ_d (upper), and on the surface charge densities for rutile at pH = 10. σ_0 is the experimental (total) surface charged density defined by Eq. (13), while σ_s is the effective surface charge density, Eq. (15). The parameters used in calculations are the same as in Fig. 5

The foregoing analysis assumed certain values for Γ_{tot} and for the electrokinetic slipping plane separation. The uncertainty in these parameters does not affect the above conclusions; it only changes the values of other constants. For example, a lower Γ_{tot} would correspond to a higher K^0_a, but other quantities would essentially remain unchanged.

This study stresses the significance of ion association in all phenomena related to the equilibria in the electrical interfacial layer. Intuitively, one would expect such an effect, since the counterions exhibit their specificity only in the Stern layer where they interact with surface charged groups. Any specificity in the Gouy–Chapman diffuse layer should be much less pronounced. Since all colloid phenomena show the lyotropic effect, one may conclude that a substantial portion of the surface charge is compensated by bound counterions, and that the surface potential (ψ_d) significantly decreases by the addition of the electrolyte. Thus, the common assumption of the constancy of ψ_d in the coagulation region is not justified (see the upper part of Fig. 7). The total surface charge density, σ_0, an experimental quantity defined as (written for KCl)

$$\sigma_0 = F(\Gamma_{MOH_2^+} + \Gamma_{MOH_2Cl} - \Gamma_{MO^-} - \Gamma_{MOK}) \tag{14}$$

increases with electrolyte concentration (Fig. 7, lower part). In contrast, the "free" uncompensated surface charge density (σ_s), which is equivalent to the charge density in the diffuse layer (σ_d)

$$\sigma_s = -\sigma_d = F(\Gamma_{MOH_2^+} - \Gamma_{MO^-}) \tag{15}$$

remains approximately constant (up to $10^{-2}\,mol\,dm^{-3}$) and then gradually decreases. The differences between σ_0 and σ_s represent the concentrations of the surface charged groups associated with counterions.

In conclusion, it may be stated that counterions of the type Li^+, K^+, or Cs^+ are bound electrostatically to charged surface groups (MO^-), generated by dissociation of protons from the surface MOH-sites. The association becomes significant at $pH > pH_{zpc}$ due to the "overall" negative surface potential. In the vicinity of the zpc the binding is negligible and $pH_{zpc} = pH_{iep}$. This behavior differs from species which can form a strong chemical bond with the surface groups, such as imidodiacetic acid anion, in which case there is a significant difference in the iep and zpc values [26].

Acknowledgements

Partial support of this research by the Bureau of Mines through a grant (Grant No. G1174106) to the California MMRRI and by the NSF Grant CHE-9108420 is acknowledged.

References

1. Fuerstenau DW, Manmohan D, Raghavan S (1981) In: Tewari PH (ed) The Adsorption of Alkaline-Earth Metal Ions at the Rutile/Aqueous Solution Interface, Adsorption from Aqueous Solutions, Plenum Publishing Corporation, New York
2. Dumont F, Warlus J, Walillon A (1990) J Colloid Interface Sci 138:543
3. Čolić M, Fuerstenau DW, Kallay N, Matijević E (1991) Colloids Surf 59:169
4. Robinson RA, Stokes RH (1955) Electrolyte Solutions. Butterworths, London
5. Bjerrum N (1926) Ergeb Exakten Naturwiss 6:125
6. Kallay N, Tomić M (1988) Langmuir 4:559
7. Tomić M, Kallay N (1988) Langmuir 4:565
8. Huang CP, Stumm W (1973) J Colloid Interface Sci 43:409
9. Warszyński P, van de Ven TGM (1990) Faraday Discuss Chem Soc 90:313
10. Stumm W, Huang CP, Jenkins SR (1970) Croat Chem Acta 42:223
11. Schindler PW, Gamsjäger H (1972) Kolloid Z u Z Polymere 250:759
12. Yates DE, Levine S, Healy TW (1974) J Chem Soc Faraday Trans I 70:1807
13. Davis JA, James RO, Leckie JO (1978) J Colloid Interface Sci 63:480
14. Blesa MA, Kallay N (1988) Adv Colloid Interface Sci 28:111
15. Kallay N, Sprycha R, Tomić M, Žalac S, Torbić Ž (1990) Croat Chem Acta 63:467
16. Hesleitner P, Babić D, Kallay N, Matijević E (1987) Langmuir 4:815
17. Hesleitner P, Kallay N, Matijević E (1991) Langmuir 7:178, 1554
18. Kallay N, Hlady V, Jednačak-Bišćan J, Milonjić S (1993) In: Rossiter BW, Baetzold RC (eds) Techniques for the Study of Adsorption from Solution, Investigation of Surfaces and Interfaces, Part A, Vol IXA of: Physical Methods of Chemistry Series, Wiley, New York, Chap. 2, Second Edition
19. Anderson MA, Rubins AJ (eds) (1981) Adsorption of Inorganics at Solid Liquid Interfaces. Ann Arbor Science, Ann Arbor, Michigan
20. Kallay N, Babić D, Matijević E (1986) Colloids Surf 19:375
21. Bérubé Y, de Bruyn PL (1968) J Colloid Interface Sci 28:92
22. Sprycha R (1984) J Colloid Interface Sci 102:173
23. Visser J (1972) Adv Colloid Interface Sci 3:331
24. Hogg R, Healy TW, Fuerstenau DW (1966) Trans Faraday Soc 62:1638
25. Kallay N, Biškup B, Tomić M, Matijević E (1986) J Colloid Interface Sci 114:357
26. Torres R, Kallay N, Matijević E (1988) Langmuir 4:706

Received June 8, 1993;
accepted June 9, 1993

Authors' address:

Dr. E. Matijevic
Center for Advanced Materials Processing
Clarkson University
Box 5814
Potsdam, NY 13699-5814, USA